Fermi National Accelerator Laboratory

FERMILAB-Conf-93/203-E

CDF

Probing the Gluon Distribution with the SS-OS Dijet Cross-Section Ratio

The CDF Collaboration

Fermi National Accelerator Laboratory
P.O. Box 500, Batavia, Illinois 60510

August 1993

Submitted to the *International Symposium on Lepton and Photon Interactions*, Cornell University, Ithaca, New York, August 10-15, 1993

Operated by Universities Research Association Inc. under Contract No. DE-AC02-76CHO3000 with the United States Department of Energy

Disclaimer

CDF/PUB/JET/PUBLIC/2163
FERMILAB-CONF-93/203-E

Probing the Gluon Distribution with the SS-OS Dijet Cross-Section Ratio

The CDF Collaboration

Abstract

We present a measurement of the same-side to opposite-side dijet cross-section ratio in $p\bar{p}$ collisions at $\sqrt{s} = 1.8$ TeV, using approximately $9.4pb^{-1}$ of data collected by the Collider Detector at Fermilab during the 1992-93 run of the Fermilab Tevatron. We show that, for large pseudorapidities and small transverse energies, this ratio is sensitive to the gluon distribution function evaluated at small x. Our measurement shows evidence for a singular gluon distribution in this region.

Submitted International Symposium on Lepton and Photon Interactions, Cornell University, Ithaca, NY, August 10-15, 1993

1 Introduction

With the advent of next-to-leading order QCD calculations for many hadronic processes[1], the lack of precise knowledge of the behavior of the gluon distribution function, particularly at small momentum fraction x, has become one of the biggest theoretical uncertainties in performing precision tests of QCD at $p\bar{p}$ colliders. Furthermore, recent advances in soft-gluon resummation techniques have yielded quantitative predictions for the small-x behavior of the gluon distribution[2], and provide strong motivation for finding new methods to probe directly the value of the gluon distribution function at small x.

In this paper, we present preliminary results for a measurement of R, the ratio of the "same-side" (SS) and "opposite-side" (OS) two-jet differential cross sections for jet production in $p\bar{p}$ collisions at $\sqrt{s} = 1800$ GeV. The same-side (opposite-side) jet cross section is obtained by selecting events having jet configurations for which η_1 and η_2, the pseudorapidities of the two jets with the highest transverse energies, have the same absolute values and the same (opposite) signs. That is, the two leading jets are required to be on the same (opposite) side of the detector at the same value of $|\eta|$. This ratio has a number of advantages, both experimental and theoretical. Experimentally, some systematic errors, such as the normalization error on the luminosity and errors due to trigger efficiency corrections will cancel. Furthermore, since the ratio of the cross sections varies much more slowly with E_T than the cross section itself, the ratio is relatively insensitive to energy-resolution smearing effects. Theoretically, for cases where both jets have low values of transverse energy, E_T, and high values of $|\eta|$, the ratio provides a direct and sensitive probe of the value of the gluon distribution at small x.

We can understand the small-x sensitivity of R by appealing to arguments based on LO QCD. For $2 \to 2$ scattering, given the transverse momentum p_T and the rapidities y_1 and y_2 of the two final state partons, one can readily deduce the momentum fractions x_a and x_b of the incoming partons:

$$x_{a,b} = \sqrt{\tau}\exp(\pm y_{boost}), \tag{1.1}$$

where

$$\sqrt{\tau} = (2p_T/\sqrt{s})\cosh y^*, \tag{1.2a}$$

$$y^* = \tfrac{1}{2}(y_1 - y_2), \tag{1.2b}$$

$$y_{boost} = \tfrac{1}{2}(y_1 + y_2). \tag{1.2c}$$

Identifying the final state partons with the outgoing jets, we find that at CDF, by choosing jet configurations with $y_1 = y_2 = 2.5$, and $p_T = 20$ GeV, values as small as $x = .002$ can be easily reached. Schematically, the two-jet differential cross section may be written as

$$\frac{d\sigma}{dy_1 dy_2 dp_T} \sim \sum_{ij} f_i(x_a, Q^2) f_j(x_b, Q^2) \hat{\sigma}_{ij}(p_T, y^*), \tag{1.3}$$

where the $f_i(x, Q^2)$ denote the parton distribution functions for partons of type i ($i = u$, $\bar{u}$, ...) evaluated at momentum fraction x and momentum scale Q, and the $\hat{\sigma}_{ij}$ denote the parton-parton cross sections for the scattering of partons i and j.

Now consider the ranges of the kinematic variables that are selected by choosing SS jet configurations, namely $y_{boost} = \bar{y}$ and $y^* = 0$. For large values of $|\bar{y}|$ and small values of p_T, the two-jet cross section in (1.3) is sensitive to the product of parton distributions, one evaluated at large x, $x_a = (2p_T/\sqrt{s})\exp(|\bar{y}|)$, and the other evaluated at small x, $x_b = (2p_T/\sqrt{s})\exp(-|\bar{y}|)$. Hence, for sufficiently extreme values of $|\bar{y}|$ and p_T, we expect the sum in (1.3) to be dominated by the contributions from gluon–valence-quark scattering. Since the valence-quark distributions are well known at large x, the SS cross section is a direct measure of the gluon distribution at small x. On the other hand, by choosing OS jet configurations, we select $y_{boost} = 0$ and $y^* = \bar{y}$. Then, the two-jet cross section is sensitive to the product of parton distributions both evaluated at $\bar{x} = (2p_T/\sqrt{s})\cosh\bar{y} = 1/2(x_a + x_b)$. The dominant subprocess contributing to the sum in (1.3) is either gluon-gluon or gluon-quark scattering, depending on the precise value of $\bar{x}$; however for region of greatest interest to us, $\bar{x}$ is large, and the parton distributions are relatively well known. Hence, at large $|\bar{y}|$, R can be approximated by

$$R \sim FG(2p_T/\sqrt{s}\exp(-\bar{y}), p_T^2), \tag{1.4}$$

where $G(x, Q^2)$ denotes the gluon distribution function, and F represents a known function of p_T and $\bar{y}$. We see from (1.4) that if the gluon distribution is singular at small x, then as $\bar{y}$ is increased, the prediction for R should grow more rapidly than the prediction for a nonsingular gluon distribution.

2 Data Analysis

For this analysis, we use approximately $9.4pb^{-1}$ of data collected by the CDF Collaboration during the 1992-93 run of the Fermilab Tevatron $p\bar{p}$ Collider. The CDF detector and trigger system have been described in detail elsewhere.[3, 4, 5] Here, we note only those changes relevant to this analysis. For the 1992-93 run, in order to span a large range of cross sections, four separate thresholds of 20, 50, 70 and 100 GeV were imposed on the E_T of the trigger clusters. The three lowest thresholds were prescaled to accept 1 in 500, 1 in 20, and 1 in 6 events, respectively. Jets have been identified using the CDF jet-cone algorithm[5], with jet E_T's being measured by summing the energies inside a cone of radius $\sqrt{(\Delta\eta)^2 + (\Delta\phi)^2} = 0.7$. Backgrounds due to cosmic rays have been rejected from the samples.

In order to be included in this analysis, the events are required to pass an additional set of cuts that reject residual backgrounds and improve the quality of the data in the samples:

1. The total E_T in the event is required to be less than 2000 GeV, and the missing-E_T fraction, which is defined as the missing-E_T divided by the total E_T, is required to be less than 0.45. These cuts are designed to reject the residual cosmic rays and accelerator losses in the data samples. The upper bound on the loss of efficiency due to the application of these cuts is approximately 2%, and cancels in R.

2. The event vertex is required to be within 60 cm of the nominal interaction point. This efficiency of this cut has been measured in minimum bias data to be 94.11%.

3. Events containing only one energetic reconstructed jet are discarded by requiring that there be a second jet in the event with $E_T \geq 5$GeV .

4. A loose back-to-back cut is applied by requiring that $\Delta\phi_{12}$, the azimuthal separation between the first and second jets, lie in the range $\pi - 0.7 \leq \Delta\phi_{12} \leq \pi + 0.7$. This cut improves the data quality by reducing the background from calorimeter noise, and as discussed below, limits the size of the systematic errors on the jet-η measurements.

Sources of systematic errors on the η measurement are jet misidentification due to cracks in the detector, and η smearing effects due to QCD radiation (three jet events). Jet misidentification can occur when the second jet in the event lies near a crack in the

Sample	27–60 GeV	60–80 GeV	80–110 GeV	110–350 GeV
SS	5235	2818	2595	3117
OS	4905	2786	2696	3485

Table 1: The number of events in the SS and OS samples having a leading jet in the E_T range specified in the table.

detector. In this case, the energy of the second jet would be mismeasured. If sufficient energy is lost in the crack, the third jet may be misidentified as the second jet and *vice versa*, thereby distorting the measured η spectrum. Events of this type are preferentially rejected by the $\Delta\phi_{12}$ cut. The presence of energetic three-jet events in the sample also distorts the η spectrum. Three-jet events complicate the reconstruction of the incoming parton kinematics and can only be successfully modeled by a higher order QCD calculation. Such events should be excluded from a comparison with a LO QCD prediction, and are rejected by the $\Delta\phi_{12}$ cut. Events in which two jets have coalesced into one also fall in this category. Due to the finite cone size used in the jet-clustering algorithm, it is impossible to find two SS jets separated by less than 0.7 in ϕ. Obviously, the finite cone size does not impose such a restriction on the OS configurations. Hence, the acceptance for events in the SS sample is less than that in the OS sample. The application of the $\Delta\phi_{12}$ cut ensures that these acceptances be the same.

In order to make the experimental measurement of R, we use the variables η_1, η_2, and E_T in place of y_1, y_2 and p_T. For each event, we determine the E_T of the leading jet, and its pseudo-rapidity, η_1. Events are classified as SS configurations if η_1 and η_2 fall into the same η-bin; they are classified as OS configurations if $|\eta_1|$ and $|\eta_2|$ fall into the same η-bin, but the sign of η_1 and η_2 are opposite. Events are assigned to E_T bins based on the E_T of the leading jet. In order to improve the statistics, we choose the width of the η bins to be 0.4; the intrinsic η resolution of the CDF detector is small by comparison. The theoretical prediction for the ratio is relatively insensitive to E_T, so we choose the E_T bins to be fairly wide. The lowest E_T-value for the 20, 50 ,70 and 100 GeV data samples are chosen to correspond to the point at which the trigger becomes approximately 30% efficient for the 20 GeV data sample, and approximately 50% efficient for the others. This choice improves the statistical power of the measurement without increasing the systematic error because the trigger efficiencies cancel in the ratio of the cross sections. Table 1 gives the final number of events in each E_T bin for the SS and OS samples.

For each bin in E_T, we determine the measured values of R from the η_1 distributions for the SS and OS samples:

$$R(\eta_1, E_T) = \frac{N_{SS}(\eta_1, E_T)}{N_{OS}(\eta_1, E_T)}, \tag{2.5}$$

where $N_{SS}(\eta_1, E_T)$ and $N_{OS}(\eta_1, E_T)$ denote the number of SS and OS jet configurations with the specified kinematics, respectively. In Figs. 1–4, we show the measured values of R as a function of η_1 for the E_T ranges given in Table 1. The measured values are compared with the predictions of LO QCD, for a variety of modern parton distribution functions, and the obsolete HMRS E+ distribution, in order to illustrate the effect of a nonsingular gluon distribution on the value of R. Overall, the agreement is quite good, with some hints that the data favor a singular gluon distribution at small x. Although the measured values of R for the higher E_T ranges are not interesting from a small-x point of view, they nevertheless provide a new test of QCD in a previously unmeasured quantity.

Since the choice of p_T scale in the theoretical calculation is crucial to determining the level of agreement between the data and the prediction, some discussion of this issue is warranted. In each figure, the p_T scale that has been chosen for evaluating the QCD prediction is a very preliminary estimate of the mean true E_T that contributes to the range of measured E_T's observed in the data. The estimate is based on knowledge of how these scales have translated between each other for measurements of the inclusive-jet cross section. In Fig. 5, we illustrate the importance of the choice of p_T scale by comparing the theoretical predictions for the MRS D-$'$ parton distribution, for a range of p_T values that might be expected to contribute to the measured energy range of the data in Fig. 1. We see that there is considerable variation amongst the predictions for the η region of greatest interest to us.

We are improving the preliminary estimate of the true E_T scale that should be used in a comparison between the data and the theory, by taking into account the detector effects of energy degradation and energy resolution smearing. Such effects result in a measured jet E_T, E_T^{meas}, that is different from the true jet E_T, E_T^{true}. These energy loss and smearing effects have been studied extensively[5, 6], and quantified in the form of detector response functions $R_{CDF}(E_T^{true}, E_T^{meas})$. The response functions give the probability that a jet having some value of E_T^{true} will fluctuate to a jet with E_T^{meas} in the data. An estimate of $\bar{E}_T^{true}$, the mean value of E_T^{true} that contributes to the measured E_T bin, $E_l^{meas} \leq E_T^{meas} \leq E_u^{meas}$, can be made by folding the energy-weighted LO QCD prediction for the two-jet cross section with the detector response functions, and integrating over the allowed values of E_T^{true} and E_T^{meas}:

$$\bar{E}_T^{true} = \frac{1}{N}\int_{E_l^{meas}}^{E_u^{meas}} dE^{meas} \int_0^{\sqrt{s}/2} dE^{true} E^{true} R_{CDF}(E^{true}, E^{meas}) d\sigma(E^{true}, \eta_1, \eta_2). \qquad (2.6)$$

In (2.6), N is the normalization factor obtained by computing the integral without the energy-weighting factor in the integrand. The calculation of the $\bar{E}_T^{true}$ values is currently in progress. Preliminary results indicate that, for small values of $|\eta|$, the estimates given in Figs. 1–4 are approximately correct; for large values of $|\eta|$ however, owing to the steepening of the jet E_T spectrum in this kinematic region, resolution smearing effects become more important and $\bar{E}_T^{true}$ is shifted to a smaller value.

The effect of E_T-resolution smearing can be separately estimated by performing a toy Monte Carlo calculation: Each p_T value is smeared by a Gaussian probability distribution whose width closely approximates the known energy resolution of the CDF detector, and the number of events generated is determined by the LO QCD prediction for the unsmeared p_T. Preliminary results indicate that, for $|\eta| \lesssim 2$, the shift in the smeared values of R is found to be small. This behavior is expected because, unlike the inclusive jet-E_T spectrum, R is relatively independent of p_T for $|\eta| \lesssim 2$ (see Fig. 5), and therefore its value should be less sensitive to distortion arising from E_T-resolution smearing effects.

Another source of systematic error on the measured E_T arises from differences in the energy scales and energy resolutions between the central calorimeter ($|\eta| \leq 1.1$), and the plug ($1.1 \leq |\eta| \leq 2.2$) or forward ($2.2 \leq |\eta| \leq 4.2$) calorimeters. From dijet-balancing studies, it is known that the size of the correction to the relative E_T scale between these detector components is typically less than 10%, away from the crack regions of the detector. The effect on R is expected to be much smaller. Since we have selected the data samples so as to ensure that we do not compare the energy scales for jets on opposite sides of the detector, any asymmetry in these scales could manifest itself as an asymmetry in R. Within the statistics currently available, no such asymmetry in R is apparent in the data. Detailed studies of the effect of shifts and asymmetries in the energy scales and resolutions are in progress.

Although we expect trigger efficiency corrections to cancel in R, we have made a further check that systematic corrections for any trigger efficiency asymmetries are negligible. We find that, as we raise the lower E_T threshold of any of the measured energy ranges to the point where the trigger becomes 100% efficient, the values of R for positive and negative η agree within statistical errors.

3 Conclusions

We have presented a measurement of the SS-OS dijet cross section ratio for a wide range of measured E_T values. No corrections have been made to the data for the effects of either E_T or η smearing. We have made a preliminary estimate of the E_T scale correction factor for each measured E_T bin, and have evaluated the theoretical predictions at the corrected value of E_T. The data are consistent with the LO QCD predictions for the values of R in all of the E_T and η ranges that have been studied. At present, the measurement is limited by low statistics. Although the data are unable to discriminate amongst the modern parton distributions, one can see that the obsolete non-singular gluon distribution is clearly disfavored, and that there is some evidence for the singular gluon hypothesis. We expect that the remainder of the data from Run Ia will provide a reduction factor of about four in the size of the statistical error bars. Hence, in the near future, this measurement should provide a strong constraint on the behavior of the gluon distribution at small values of x.

References

[1] S. Ellis, Z. Kunszt, and D. Soper, Phys. Rev. Lett. 62, 2188 (1989); Phys. Rev. Lett. 64, 2121 (1990).

[2] E.M. Levin and M.G. Ryskin, Nucl. Phys. B (Proc.Suppl.) 18C, 92 (1991).

[3] CDF Collaboration, F. Abe *et al.*, Nucl. Istrum. Methods Phys. Res., Sect. A 271,387 (1988).

[4] CDF Collaboration, F. Abe *et al.*, Phys. Rev. Lett. 62, 613 (1989).

[5] CDF Collaboration, F. Abe *et al.*, Phys. Rev. Lett. 68, 1104 (1992).

[6] CDF Collaboration, F. Abe *et al.*, Phys. Rev. Lett. 70, 1376 (1993).

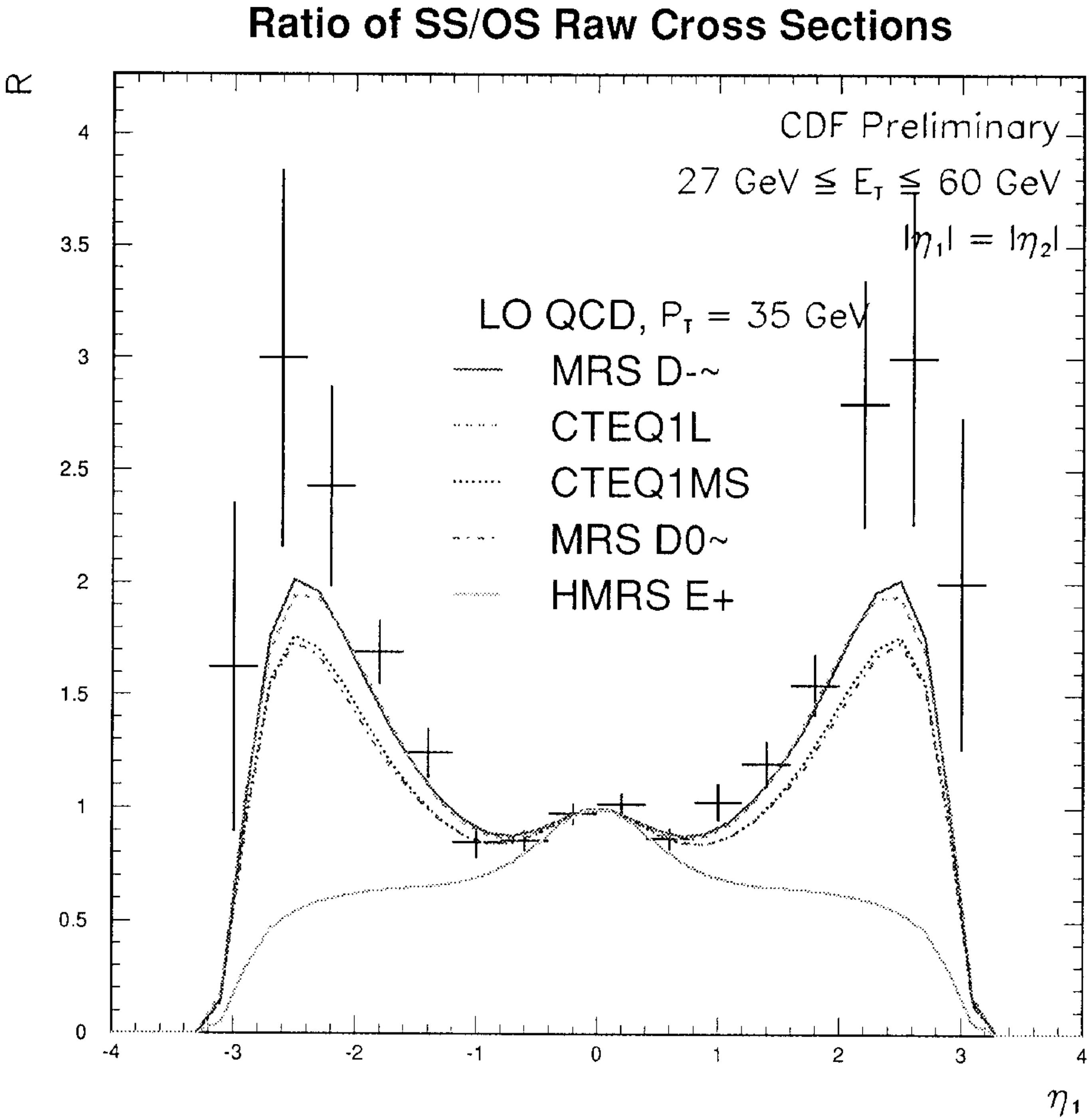

Figure 1: The measured values of R as a function of η_1 in the measured E_T range $27 \leq E_T \leq 60$ GeV.

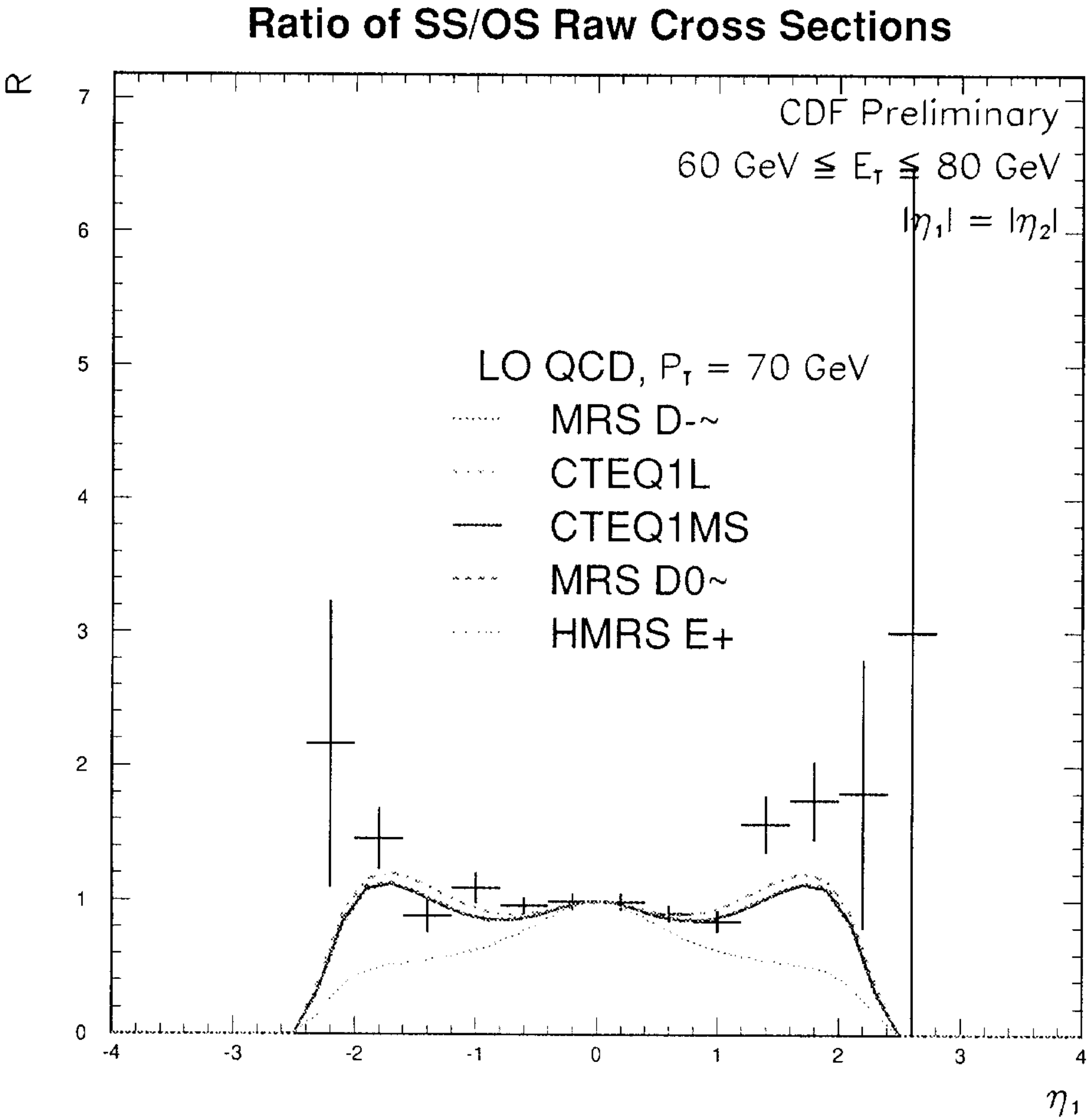

Figure 2: The measured values of R as a function of η_1 in the measured E_T range $60 \leq E_T \leq 80$ GeV.

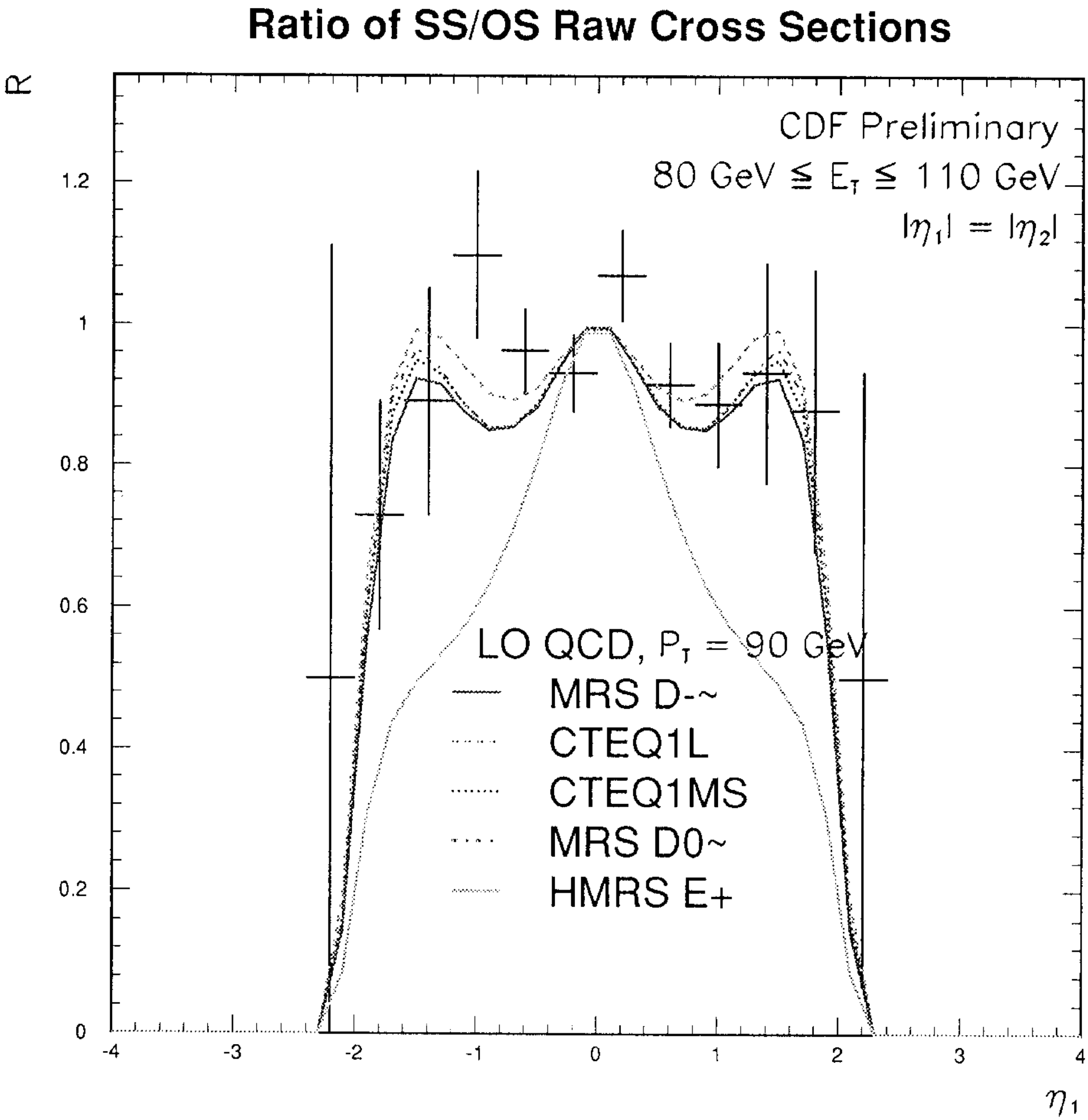

Figure 3: The measured values of R as a function of η_1 in the measured E_T range $80 \leq E_T \leq 110$ GeV.

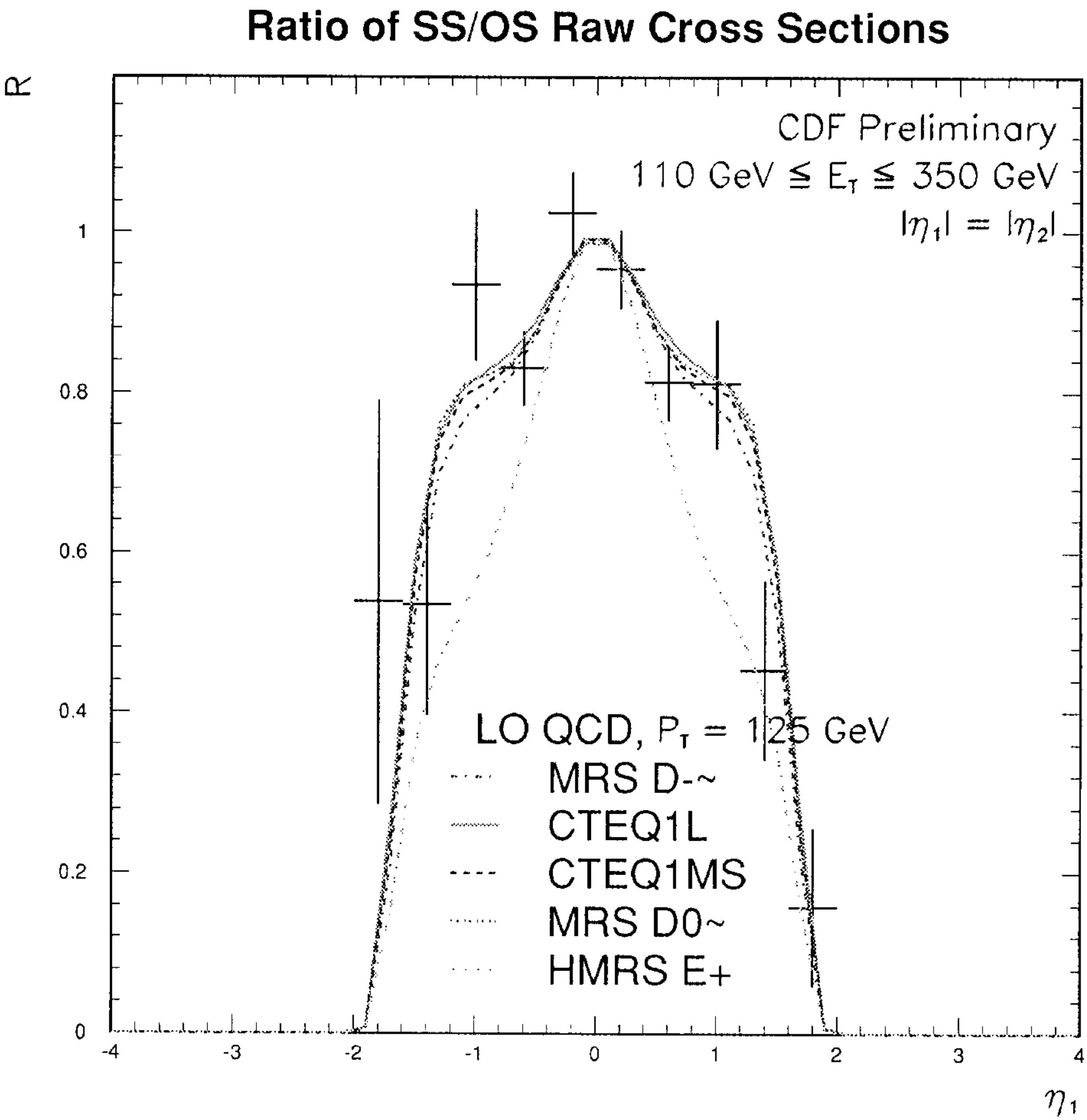

Figure 4: The measured values of R as a function of η_1 in the measured E_T range $110 \leq E_T \leq 350$ GeV.

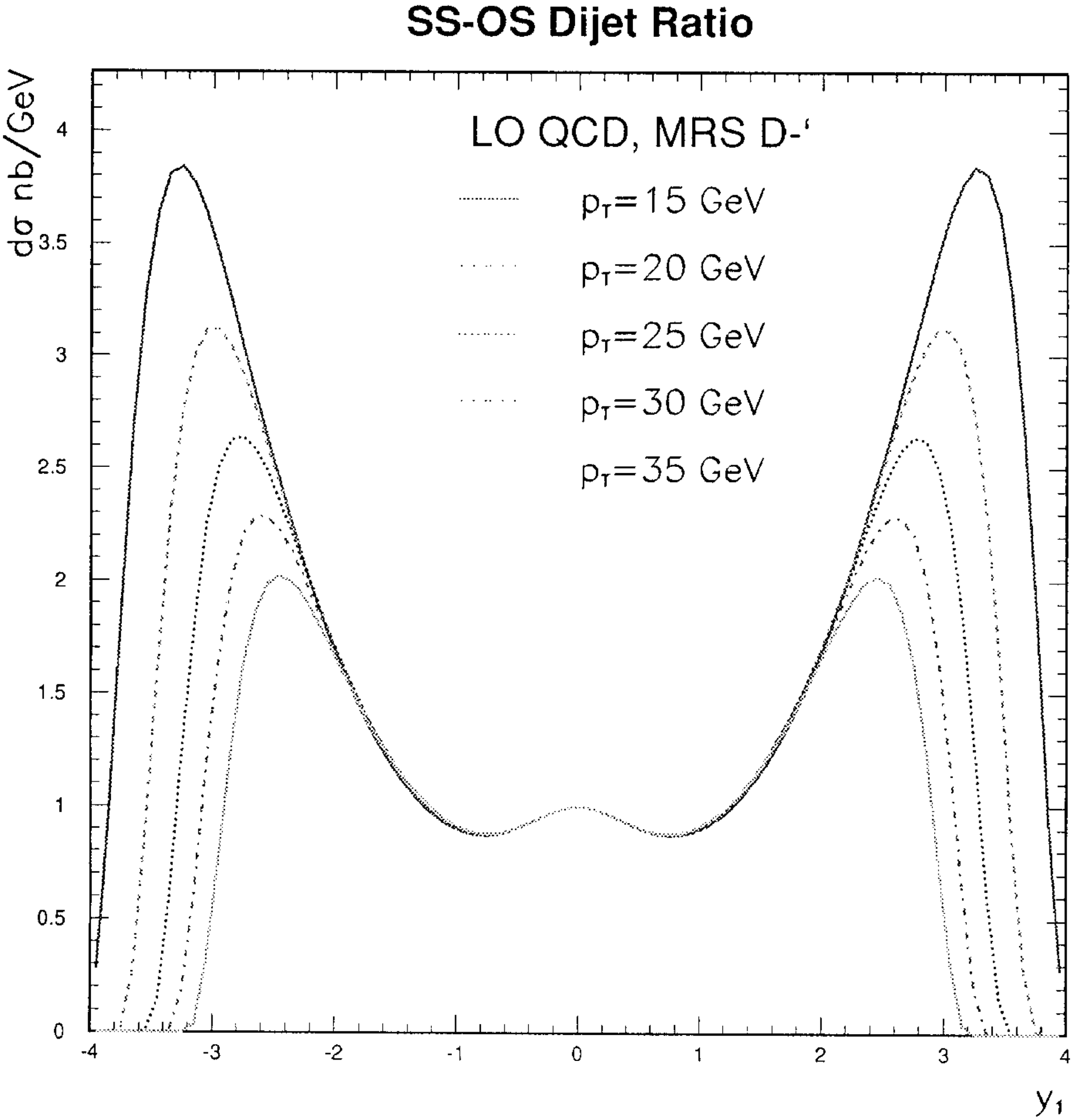

Figure 5: The variation in the LO QCD prediction for the SS-OS dijet ratio for p_T values in the range $15 \leq p_T \leq 35$ GeV. The predictions have been calculated using the MRS D-′ parton distribution.